OPEN ACCESS

# STRUCTURE OF POLYMER/CLAY NANOCOMPOSITES, A MOLECULAR MODELLING PERSPECTIVE

Nikita Siminel*, ORCID: 0000-0002-1055-7078

*Technical University of Moldova, 168 Stefan cel Mare Blvd., MD-2004, Chisinau, Republic of Moldova*
*Corresponding author, Nikita Siminel, *siminel.n@gmail.com*

**Abstract.** The search for renewable biodegradable materials to replace conventional oil-based plastics is a fast-growing research area as it provides an important factor for the sustainable growth of the packaging industry. In this regard, clay-containing composite materials have numerous current and potential commercial applications. However, the interaction between clay and polymer, i.e. Poly(ethylene glycol), is influenced by many factors, such as the nature of the clay, length and nature of the polymer chain, hence, in this work polymer/clay nanocomposite is studied both ex`perimentally and theoretically. Structural and thermodynamic properties of formulated nanocomposites are probed using XRD and TGA techniques and then compared with corresponding values derived from a series of Molecular Dynamics simulations of intercalated polymer/clay nanocomposites. For the first time, the developed potential models were able to predict realistic basal spacing of poly(ethylene glycol)/clay nanocomposite. The simulation also revealed the structure of the interlayer on a molecular level, which greatly benefited the understanding of the formation of polymer/clay coatings. The swelling dynamics, energetics and structure of the clay interlayers are examined. Particular attention is paid to the behaviour of polymer and water when they coexist in the clay interlayer.

**Keywords:** *molecular dynamics, montmorillonite, clay, water, polymer, composite, clay-coatings.*

**Rezumat.** Căutarea de materiale regenerabile biodegradabile care să înlocuiască materialele plastice convenționale pe bază de ulei este un domeniu de cercetare în ascensiune, deoarece oferă posibilitate pentru creșterea durabilă a industriei ambalajelor. În acest sens, materialele compozite care conțin argilă au numeroase aplicații comerciale actuale și potențiale. Cu toate acestea, interacțiunea dintre argilă și polimer este influențată de mulți factori, cum ar fi natura argilei, lungimea și natura lanțului polimeric. În această lucrare, nanocompozitul polimer/argilă este cercetat experimental și teoretic. Proprietățile structurale și termodinamice ale nanocompozitelor formulate sunt testate folosind tehnici XRD și TGA și ulterior comparate cu valorile corespunzătoare derivate dintr-o serie de simulări de dinamică moleculară a nanocompozitelor intercalate polimer/argilă. Pentru prima dată, modelele potențiale dezvoltate au reușit să modeleze distanța bazală realistă a nanocompozitului poli(etilen glicol)/argilă. Simularea a dezvăluit, de asemenea, structura stratului intermediar

la nivel molecular, ceea ce a avantajat înțelegerea formării acoperirilor de polimer/argilă. Se examinează dinamica gonflării, energia și structura straturilor intermediare de argilă. O atenție deosebită este acordată comportării polimerului și apei atunci când acestea coexistă în stratul intermediar de argilă.

**Cuvinte cheie:** *dinamică moleculară, montmorillonit, argilă, apă, polimer, compozit, acoperiri cu argilă.*

***Abbreviations:***

MD – Molecular Dynamics Simulation;
MC – Monte Carlo Simulation;
NaMt – $Na^+$-Montmorillonite;
CaMt – $Ca^{2+}$-Montmorillonite;
PEG – Poly(ethylene glycol)
XRD – X-ray Diffraction;
TGA – Thermogravimetric Analysis.

**1. Introduction**

One of the reasons that Clay Minerals are efficient adsorbents is that the interlayer spaces are potentially accessible not only for water molecules but for organic materials as well. Thus, it is necessary to investigate the adsorption between the layers to understand the structure of polymer/clay nanocomposite coatings.

Poly(ethylene glycol) (PEG, formula, $H-(O-CH_2-CH_2)_n-OH$) also known as poly(ethylene oxide) (PEO) or polyoxyethylene (POE) [1] is a non-toxic biodegradable polymer and is one of the most important polymers widely used in biotechnology, pharmaceutical compositions and as a food additive [2, 3]. In recent years, however, it has found popularity in biodegradable food packaging applications [4, 5] where it can be used as a plasticiser for polymer/clay-containing films which are otherwise notoriously brittle [6, 7].

The interaction between clay and polymer, i.e. PEG, is influenced by many factors, such as the nature of the clay, the length and nature of the polymer chain and any solvent present. There are different accounts of the intercalation of PEG in layered silicates in the available literature [8-11]. Studies based on X-ray diffraction propose a highly ordered polymer arrangement within the clay galleries.

One proposed structure of the intercalated PEG is a helix. In this model, the axis of the polymer chain is oriented parallel to the basal surface and exchangeable cations reside in the centre of the interlayer. It was first proposed by Ruiz-Hitzky et al. [12] and was believed to be plausible because only one plateau was observed in the adsorption isotherms, corresponding to the basal spacing of 18 Å. A second possible interlayer structure considers PEG chains to be organised in two extended chains parallel to clay surface layers. Here, exchangeable cations are also positioned in the middle of the interlayer [8, 9, 13]. Unlike the helix conformation, this model contemplates two stages of swelling depending on the amount of PEG available – a monolayer with a $d_{001}$-spacing of 14 Å and a planar bilayer with a $d_{001}$-spacing of 18 Å [4].

Using MD and MC simulations, Hackett et al. [14] showed that the intercalated PEG chains in clay-based nanocomposites were arranged parallel to the basal surface of the hectorite galleries. This structure agreed well with the results of neutron scattering

experiments, a review of which was given by Ray [15]. Further simulations of PEG/clay nanocomposites also suggested layered PEG structures [2, 9, 16-19].

Therefore, it is reasonable to take, from the literature, that PEG may adopt various conformations in the galleries of different clays. However, obtaining detailed molecular-scale insight into the structure and dynamics in the interlayer is difficult because of the static and dynamic disorder of these systems. Here, computational approaches, e.g. MD, can be highly informative, especially when considering both hydration and polymer intercalation processes simultaneously. In order to assess the ability of chosen models to simulate the swelling behaviour of PEG/Mt composite and rationalise the simulation observations, some experimental work on the swelling of various montmorillonite clays, when loaded with different amounts of PEG200, was performed.

## 2. Materials and Methods
### A. Experimental techniques

All experimental PEG/clay nanocomposites presented in this work were prepared using the solvent casting method. The bentonite clay samples, Cloisite Na$^+$ (NaMt) and Cloisite Ca$^{2+}$ (CaMt) were supplied by Southern Clay Products and used as received. The bentonite is predominantly composed of montmorillonite with CEC value of 92.5 meq/100g. PEG of molecular weight of 200 g·mol$^{-1}$ was used as supplied by Aldrich.

For the nanocomposite preparation, the concentration of each component used was based on the total solid content. 3 ± 0.001 g of clay was initially mixed with 60 ml of distilled water in a beaker and agitated for 2 hours using a magnetic stirrer. The desired amount of PEG200 (PEG200, clay=0, 3, 9, 12, 18, 27 wt%) was mixed in 20 ml of distilled water and added to the clay suspension. The PEG200/clay solution was then stirred for a further 6 hours at room temperature before being cast onto a glass slide and placed into a Petri dish. All of the suspensions were dried in an oven at 40 °C for 3 h and then left at room temperature for 12 h before being analysed by XRD, TG and TG-MS. XRD, in particular, provides evidence for the formation of intercalated systems by allowing measurement of the interlayer spacing. In this study, all XRD measurements were undertaken on a X'Pert Pro Diffractometer, Philips. A copper tube CuK$_\alpha$ (1.54186 Å) as the source of X-rays was used with current and voltage of 40 mA and 40 kV applied to it respectively. A divergent slit of 0.5° and anti scatter slit of 1° were used. Data was collected in the 2Θ range of 2-45° with step size of 0.02° and a scan time of 1 second per step. The Petri dishes containing the dispersions were used for general characterisation after grinding.

### B. Simulation details

A broad range of PEG200 and $H_2O$ concentrations, ranging from 0 to 0.35 g$_{(PEG200)}$/g$_{clay}$ (0 to ~7.1 PEG200·uc$^{-1}$) and 0 to 0.2 g$_{(H2O)}$/g$_{clay}$ (0 to ~16.5 H2O·uc$^{-1}$) respectively were used. Range of clay models utilised to simulate PEG/water/Mt intercalated nanocomposite comprised of eighteen montmorillonite models. Molecular dynamics simulations were performed using the Nosé-Hoover thermostat and DL_POLY simulation package with 1.0 ps of relaxation time. For the NPT simulations, a Nosé-Hoover barostat was utilised to control the pressure with a barostatic relaxation time of 1.0 ps. Interatomic interactions were evaluated using a time step of 0.001 ps, and three-dimensional periodic boundary conditions were employed with a cutoff at 10 Å for short-range interactions. Long-range electrostatic interactions were calculated using the Ewald summation with an accuracy of $1 \times 10^{-6}$. All MD simulations were performed at 300 K and at 1 atm for the NPT ensemble. Statistical and

atomic position data were collected over the last 1 ns of the simulation and stored every 25 ps to obtain the thermodynamic and structural properties of the simulated systems.

### 3. Results and Discussion
### A. Experimental Characterisation of PEG/water/Mt Intercalated Films

The XRD patterns for PEG/NaMt and PEG/CaMt with a range of PEG200 loadings are presented in Figure 1 and the corresponding calculated $d_{001}$-spacings are plotted in Figure 2. The diffraction profiles obtained are in very good agreement with numerous previous investigations of PEG intercalation into NaMt [8, 10, 11]. The shift of the XRD peak positions for $Na^+$ exchanged clay (Fig. 1(a)) indicates the presence of intercalated structures for the whole range of PEG loadings. Even a very small amount of PEG200 (3 wt%) forces the clay layers to expand from 12.7 Å to 13.6 Å (6.98° 2Θ and 6.46° 2Θ respectively). This continues with higher loadings of PEG which gradually fills the interlayer until a complete PEG200 monolayer in the interlayer is apparently formed at 12 wt% (6.22° 2Θ) with a d-spacing of ~14.4 Å (Fig. 2(a)). Further loading of PEG200 (18 wt%) results in the formation of two coexisting structures – monolayer (14.4 Å) and bilayer (16.7 Å) which are apparent from the two peaks in the XRD trace at 6.1° 2Θ and 5.1° 2Θ respectively. The bilayer polymer structure is completely formed when the PEG200 loading reaches 27 wt%, as evidenced by the narrow distribution of d-spacings and the high intensity of the XRD peak, corresponding to a d-spacing of 18.5 Å.

XRD traces suggest completely different behaviour for the $Ca^{2+}$ exchanged clay upon intercalation of PEG200 (Fig. 1(b)).
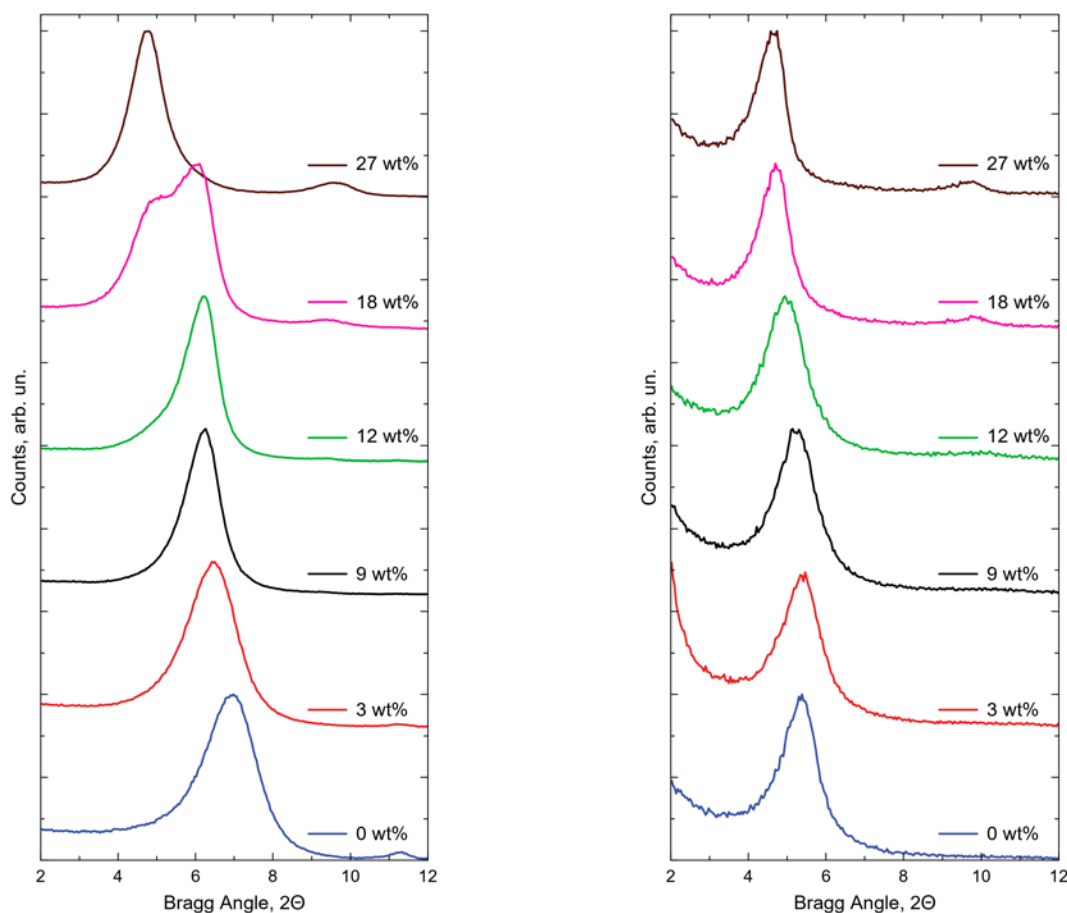


**Figure 1.** XRD patterns of PEG/Mt with 0–27 wt% PEG200 for a) $Na^+$-cloisite and b) $Ca^{2+}$-cloisite.

The XRD peak for the sample with 0 wt% PEG200 is located at 5.68° 2Θ which corresponds to d-spacing of 15.1 Å (Fig. 2(b)). At this point, only water and hydrated $Ca^{2+}$ cations are present in the interlayer. The calculated d-spacing agrees with that of the simulated clay + water systems where it was concluded that CaMt always forms a bilayer hydrate interlayer at ambient conditions, due to the high hydration capability of bivalent the exchange cation. Upon introducing PEG200 into this system, the d-spacing of PEG/CaMt increases nearly linearly until it reaches a spacing of 18.8 Å at 18 wt%. It then levels off, presumably showing the limit of intercalation capability of $Ca^{2+}$-cloisite at room temperature and normal pressure.
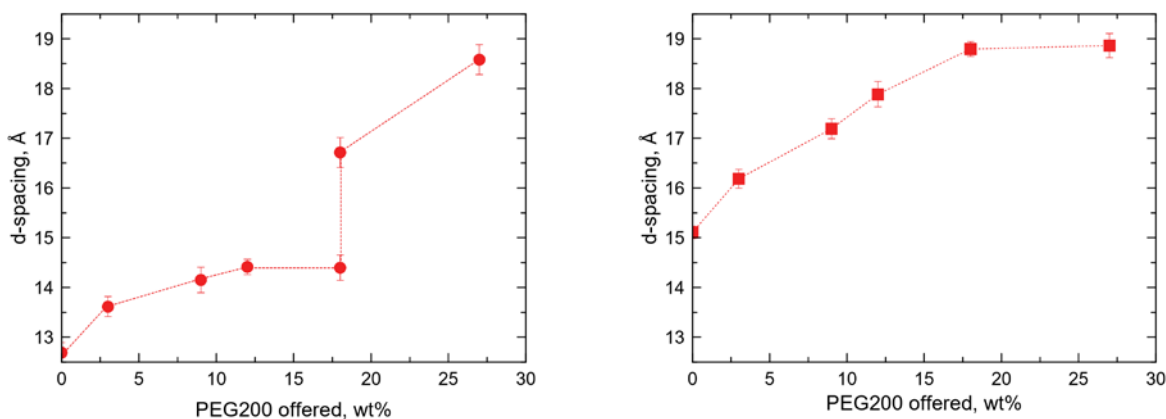


**Figure 2.** Summary of d-spacing observed in the XRD traces of PEG200/Mt for a) $Na^+$-cloisite and b) $Ca^{2+}$-cloisite.

**Thermal Decomposition of PEG in Nanocomposites**

The thermal stability of the formulated samples was investigated using the TGA technique. The thermograms (TG) and corresponding negative derivatives (dTG) for PEG/Mt nanocomposites are presented in Figures 3 and 4 and were utilised to quantify the amount of intercalated PEG and water present in the nanocomposites. Thermal decomposition of the PEG/Mt nanocomposites proceeds as a multiple-step process, (i) weight loss due to the release of water at a temperature less than 225°C; (ii) decomposition of polymer at 250–400°C forming monomers, small oligomers, and other decomposition products [8]; (iii) dehydroxylation of the Mt layer at ~ 700°C. These three processes are intrinsic for both $Na^+$ exchanged and $Ca^{2+}$ exchanged montmorillonites, as revealed by the TG curves shown in Figures 3(a) and 3(b) respectively.

The first major weight loss occurs between 35 and 150°C. The reciprocal dTG peak denoted as 1st peak in Figures 4(a) and 4(b), corresponds to the removal of water from the samples. The amount of released water decreases as the PEG concentration increases from 0 to 27 wt% (Fig. 4(a) and 4(b), 1st peak). This indicates that either some of the water present in clay is being replaced by PEG200 [10] or that more compact water aggregates are created which remain in place up to ~ 150°C [11]. A shoulder at ~ 140°C in dTG curve of pure $Ca^{2+}$-cloisite (Fig. 4(b)) is due to the decomposition of the relatively strong $Ca^{2+}$ hydration shells [8].

Adding as little as 3 wt% of PEG200 to both clays reveals a 2nd weight loss peak between 300°C and 400°C (Fig. 4). The intensity of this peak increases as the amount of PEG in the nanocomposite increases – significantly, up to 7x for NaMt but to a much smaller extent for CaMt (up to 1.5x). The weight loss curves associated with the 2nd dTG peak (Fig. 4) correlate clearly to the shapes and progression of the corresponding XRD swelling curves

(Fig. 2). In particular, the weight loss curves of PEG/NaMt nanocomposites level off between 12 and 18 wt% PEG200 content, which corresponds to a monolayer polymer organisation within the interlayer. Further increase in PEG content results in a significant increase in the weight loss associated with this. The corresponding weight loss of the CaMt-based nanocomposites, on the other hand, reaches a plateau at a lower PEG200 content which corresponds to the formation of a PEG200 bilayer in the interlayer. Similar to the swelling curve, a further increase in PEG200 content does not influence the observed weight loss.
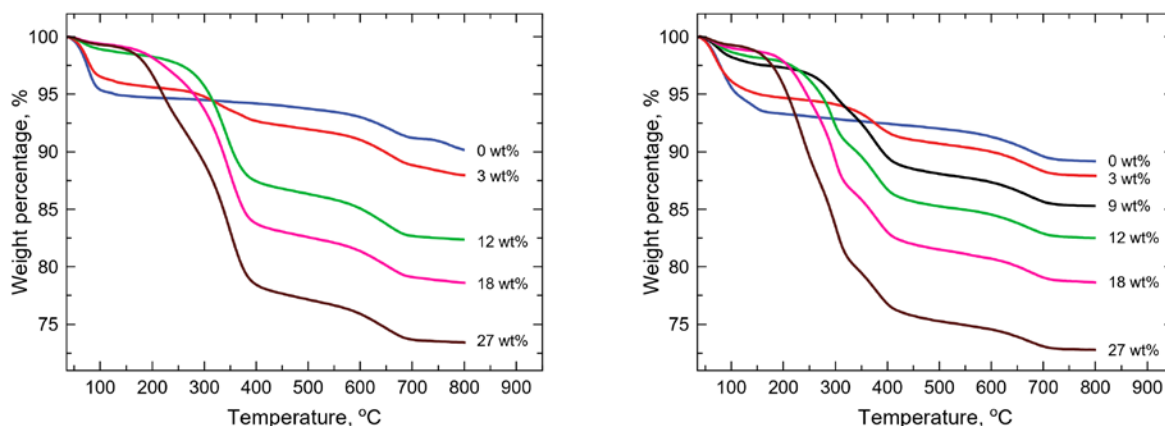


**Figure 3.** Thermograms of PEG200/Mt with different wt% PEG200 for a) Na+-cloisite and b) Ca$^{2+}$-cloisite.
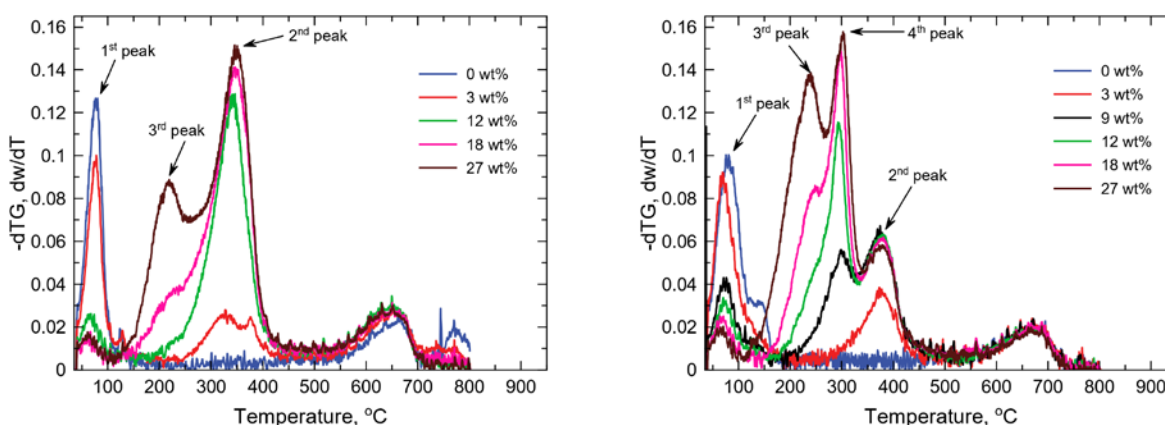


**Figure 4.** TGA negative derivatives of PEG200/Mt with different wt% PEG200 for a) Na+-cloisite and b) Ca2+-cloisite.

The third peak (Fig. 4(a)) becomes sizeable at PEG200 contents of 18 wt% for NaMt and 12 wt% for CaMt. These loadings correspond to the formation of the bilayer interlayer structure for clays in both exchanged forms (Fig. 2(a)). The weight losses at these corresponding temperatures are nearly linear, especially at high PEG content. One explanation of the 3rd weight loss peak could be not fully intercalated PEG, in which only a few polymer chain segments are occluded by the gallery and the bulk of each molecule remains in solution [9].

The amounts of water and PEG200 for all studied samples, calculated on the basis of TG curves and TGMS analysis, are presented in Table 1. Only the 1$^{st}$, 2$^{nd}$ and 3$^{rd}$ weight loss peaks (Fig. 4) were taken into account here. It is rather important to recognise that these values do not relate exclusively to intercalated media, as there is no direct way to distinguish intercalated from supernatant adsorption configurations. CaMt retained a higher amount of water for all studied samples, as expected from hydration analysis. For example, pure NaMt

and CaMt contained 5.0% and 7.3% of water respectively. NaMt, on the other hand, adsorbed higher amounts of polymer, giving adsorbed PEG loadings very close to the percentages of offered polymer. As the PEG content in the nanocomposite increased the amount of water decreased for both exchanged clay forms. This suggests that PEG intercalates by replacing the free water molecules in the gallery as well as some water that is directly coordinated to the exchangeable cations.

*Table 1*
**Amounts of PEG and water adsorbed from water solution on NaMt and CaMt, as determined by thermogravimetry**

| PEG200 offered (wt%) | NaMt | | CaMt | |
|---|---|---|---|---|
| | $H_2O$ amount (%) | PEG amount (%) | $H_2O$ amount (%) | PEG amount (%) |
| 0 | 5.0 | - | 7.3 | - |
| 3 | 4.1 | 3.8 | 5.4 | 2.7 |
| 12 | 1.2 | 10.2 | 2.2 | 9.1 |
| 18 | 0.5 | 17.3 | 1.5 | 15.8 |
| 27 | 0.4 | 23.6 | 1.1 | 21.0 |

**Computational simulation of polymer/clay nanocomposite**

Figure 5 presents the results of a series of simulations for the intercalation of PEG200 in the montmorillonite exchanged by $Na^+$ and $Ca^{2+}$ cations. The calculated basal spacing of the clay complex is plotted as a function of polymer content along with experimental data presented previously in this chapter. Carefully selected variable amounts of water in the interlayer were based on experimental data obtained from TGA and TGMS calculations (Table 1). The simulations correctly predict a step-wise swelling behaviour for NaMt. Two plateaux around PEG200 contents of 0.10 and 0.25 gPEG200/gclay are observed (Fig. 5(a)), which supports interlayer polymer organisation in two extended layers parallel to the clay surfaces – monolayer and bilayer.
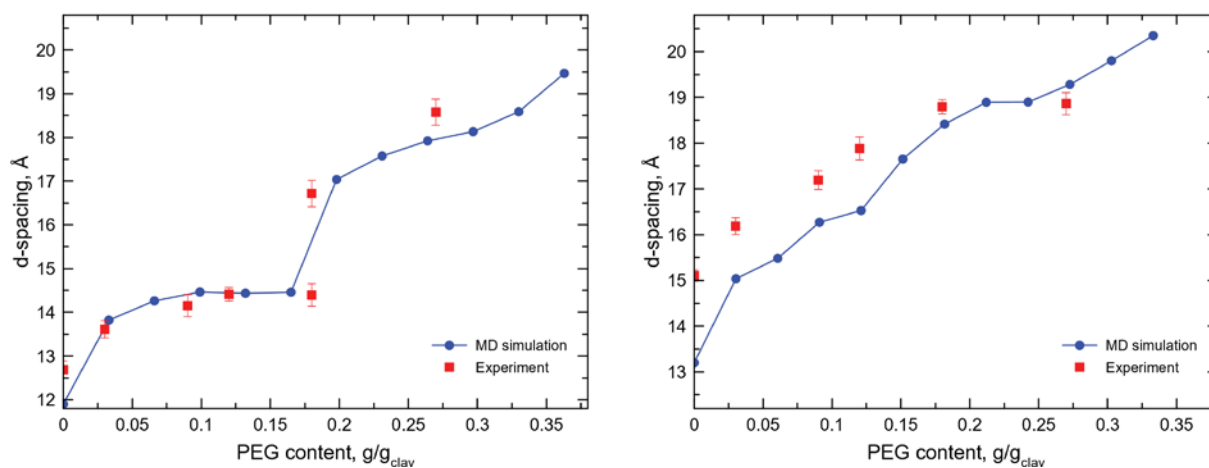


**Figure 5.** Simulated and experimental basal spacing of (a) NaMt and (b)CaMt as a function of increasing poly(ethylene glycol) (PEG200) content in the interlayer. Amount of water in the interlayer was selected according to experimental findings presented in Table 1.

More importantly, for the first time we have achieved realistic basal spacings from simulation for these two polymer arrangements. The first plateau on the swelling curve corresponds to a monolayer organisation of polymer with a d-spacing of 14.5 Å. This is an excellent match to the experimental observations presented in the previous section as well as previous experimental investigations. [7-9]. The simulated spacing that corresponds to the bilayer polymer structure is approximately 0.5 Å smaller than that obtained experimentally.

Similar to the clay hydration process, the exchangeable cation affects intercalation of PEG significantly (Fig. 5(b)). CaMt exhibits a nearly linear increase in d–spacing with the uptake of PEG200 until reaching a plateau at around 0.2–0.25 gPEG200/gclay with a spacing of 18.8 Å. This plateau corresponds to the formation of a bilayer polymer structure and again matches experimental observations. At lower polymer content, the swelling curve for CaMt is less accurate than for NaMt, however, the nearly linear swelling trend is similar to that observed experimentally. The absence of a stable monolayer polymer structure in the interlayer suggests that the level of uptake of PEG200 by CaMt is smaller when compared to that by NaMt. Similar behaviour was observed experimentally, where the ratio of the uptake of PEG1500 by NaMt to that by CaMt has been found to be about 2.3 [24].

## 4. Conclusions

Two types of commercially available bentonite clay were used to produce intercalated polymer/clay nanocomposites with a wide range of PEG and water concentrations. This was done to provide an evidence base for direct comparison with computer simulations of similar systems. Also, additional information on the processes involved in the collaborative intercalation of water and PEG into clay mineral was required. Through the use of XRD analysis, particular attention was paid to the interlayer structure of the formulated samples. Thermal stability and quantitative analysis of adsorbed organic material were assessed by TG and TGMS analysis.

XRD analysis indicated significant expansion of both clays studied upon increase of polymer content. Two stable polymer structures within the interlayer of NaMt were identified – a monolayer and a bilayer. The exchangeable cation has a significant effect on the expansion properties of montmorillonite. CaMt did not produce a stable monolayer, showing a linear increase of basal spacing as the polymer content in the system increased, until a stable bilayer polymer structure was created. The value of the d-spacing at 0 wt% of PEG200 was on par with that found in the simulations of the hydration process of clay layers, indicating the presence of a bilayer hydrate in the CaMt interlayer even at low relative humidity.

Experimental measurements of intercalated PEG/Mt nanocomposites showed that polymer chains replace some of the adsorbed water, filling the space between hydrated exchangeable cations. The amount of polymer adsorbed is influenced by the hydration enthalpy of the exchangeable cation, indicating possible associations between those exchangeable cations and the ether oxygen atoms of PEG chains. It was established that the uptake of PEG200 by NaMt is higher than that by CaMt.

The computational model of PEG200/Mt nanocomposites has proved both experimentally and theoretically to be successful at reproducing the structural and thermodynamic properties of all studied nanocomposites. It was shown that polymer chains replace some of the adsorbed water, filling the space between hydrated exchangeable cations. The amount of polymer adsorbed is controlled by the hydration enthalpy of the

exchangeable cation, indicating possible associations between the exchangeable cation and the ether oxygen atoms of the PEG chains. It was also found that montmorillonite mineral preferentially absorbs the high molecular weight fractions of PEG. From an engineering point of view, these results are significant because they suggest that nanocomposites with better barrier and mechanical properties could be obtained by controlling molecular weight distribution to avoid low polymer fractions.

**Conflicts of Interest.** The author declares that they have no conflict of interest.

### References

1. Wang, Q.; Keffer, D.J.; Nicholson, D.M. A coarse-grained model for polyethylene glycol polymer. J. Chem. Phys 2011, 135(21), 214903
2. Krishnan, M.; Saharay, M.; Kirkpatrick, J.R. Molecular dynamics modeling of $CO_2$ and poly(ethylene glycol) in montmorillonite, the structure of clay/polymer composites and the incorporation of $CO_2$. J. Phys. Chem. C, 2013, 117, 20592–20609.
3. Adams, M.L.; Lavasanifar, A.; Kwon, G.S. Amphiphilic block copolymers for drug delivery. J. Pharm. Sci., 2003, 92(7), 1343–1355.
4. Johansson, C.; Bras, J.; Mondragon, I.; Nechita, P.; Plackett, D.; Simon, P.; Svetec, D.G.; Virtanen, S.; Baschetti, M.G.; Breen, C.; Clegg, F.; Aucejo, S. Renewable fibers and bio-based materials for packaging applications - a review of recent developments. Bioresources, 2012, 7(2), 2506–2552.
5. Barish, J.A.; Goddard, J.M. Polyethylene glycol grafted polyethylene, a versatile platform for nonmigratory active packaging applications. J. Food Sci., 2011, 76(9), E586–91.
6. Rodriguez-Llamazares, S.; Rivas, B.L.; Perez, M.; Perrin-Sarazin, F. Poly(ethylene glycol) as a compatibilizer and plasticizer of poly(lactic acid)/clay nanocomposites. High Perform. Polym., 2012, 24(4), 254–261.
7. Clegg, F.; Breen, C.; Khairuddin. Synergistic and competitive aspects of the adsorption of poly(ethylene glycol) and poly(vinyl alcohol) onto Na-bentonite. J. Phys. Chem. B, 2014, 118(46), 13268–13278.
8. Bujdák, J.; Hackett, E.; Giannelis, E.P. Effect of layer charge on the intercalation of poly(ethylene oxide) in layered silicates, implications on nanocomposite polymer electrolytes. Chem. Mater., 2000, 12(8), 2168–2174.
9. Chen, B.; Evans, J.R.G., Greenwell, C.H.; Boulet, P.; Coveney, P.V.; Bowden, Al.A; Whiting, A. A critical appraisal of polymer-clay nanocomposites. Chem. Soc. Rev., 37(3), 568–94, mar 2008.
10. Khairuddin. Clay-polyvinylalcohol nanocomposites, competitive adsorption of polyvinylalcool and plasticiser onto Na-bentonite. PhD thesis, Sheffield Hallam University, Sheffield, UK, 2012.
11. Chen, B. Polymer-clay nanocomposites. PhD thesis, Queen Mary University of London, London, UK, 2004.
12. Ruiz-Hitzky, E.; Aranda, P. Polymer-salt intercalation complexes in layer silicates. Adv. Mater., 1990, 2(11), 545–547.
13. Chen, B. Polymer-clay nanocomposites, an overview with emphasis on interaction mechanisms. Br. Ceram. Trans., 2004, 103(6), 241–249.
14. Hackett, E.; Manias, E.; Giannelis, E.P. Computer simulation studies of PEO/layer silicate. Chem. Mater., 12(8), 2000, 2161–2167.
15. Sinha, R. S.; Okamoto, M. Polymer/layered silicate nanocomposites, a review from preparation to processing. Prog. Polym. Sci., 2003, 28(11), 1539–1641.
16. Mazo, M.A.; Manevitch, L.I.; Gusarova, E.B.; Shamaev, M.Yu.; Berlin, A.A.; Balabaev, N.K.; Rutledge, G.C. Molecular dynamics simulation of thermomechanical properties of montmorillonite crystal. 3. Montmorillonite crystals with PEO oligomer intercalates. J. Phys. Chem. B, 2008, 112, 3597–3604.
17. Mazo, M.A.; Manevitch, L.I.; Gusarova, E.B.; Berlin, A.A.; Balabaev, N.K.; Rutledge, G.C. Molecular dynamics simulation of thermomechanical properties of montmorillonite crystal. II. Hydrated montmorillonite crystal. J. Phys. Chem. C, 2008, 112, 17056–17062.
18. Siqueira, L.J.A.; Ribeiro, M.C.C. Molecular dynamics simulation of the polymer electrolyte poly(ethylene oxide)/LiClO(4). II. Dynamical properties. J. Chem. Phys, 2006, 125(21), 214903.

19. Suter, J.L.; Coveney, P.V. Computer simulation study of the materials properties of intercalated and exfoliated poly(ethylene)glycol clay nanocomposites. Soft Matter, 2009, 5(11), 2239.
20. Chen, B.; Evans, J.R.G. Preferential intercalation in polymer-clay nanocomposites. J. Phys. Chem. B, 2004, 108(39), 14986–14990.
21. Ottani, S.; Vitalini, D.; Comelli, F.; Castellari, C. Densities, viscosities, and refractive indices of poly(ethylene glycol) 200 and 400 + cyclic ethers at 303.15K. J. Chem. Eng. Data, 2002, 47(5), 1197–1204.
22. Lee, H.; Venable, R.M.; Mackerell, A.D.; Pastor, R.W. Molecular dynamics studies of polyethylene oxide and polyethylene glycol, hydrodynamic radius and shape anisotropy. Biophys. J., 2008, 95(4), 1590–1599.
23. Waggoner, R.A.; Blum, F.D.; Lang, J.C. Diffusion in aqueous solutions of poly(ethylene glycol) at low concentrations. Macromolecules, 1995, 28(3), 2658–2664.
24. Parfitt, R.L.; Greenland, D.J. Adsorption of water by montmorillonitepoly (ethylene glycol) adsorption products. Clay Miner., 1970, 317.

**Submission of manuscripts**:                                    jes@meridian.utm.md